

Effect of Residual Stresses on Wave Propagation in Adhesively Bonded Multilayered MEMS Structures

M. Kashtalyan^{1,2} and Y.A. Zhuk³

Abstract: The paper investigates propagation of stationary plane longitudinal and transverse waves along the layers in adhesively bonded multilayered structures for MEMS applications in the presence of residual stresses. The multilayered structure is assumed to consist of the infinite amount of the periodically recurring layers made of two different materials possessing significantly dissimilar properties: conductive metal layer and insulating adhesive layer. It is assumed that the mechanical behaviour of both materials is nonlinear elastic and can be described with the help of the elastic Murnaghan potential depending on the three invariants of strain tensor. The problem is formulated in the framework of the three-dimensional linearized elasticity theory of finite initial deformations. The influence of the residual stresses in each layer and of the ratio of the layer thicknesses on the normalized velocity of propagation of the stationary plane wave is examined and discussed. It is found that for some multilayered structures there exist such values of the ratio of the layer thicknesses that wave velocities do not depend on the magnitude of residual stresses but are equal to the corresponding wave velocities in the unstressed structure.

Keywords: microelectromechanical systems, multilayered structure, three-dimensional linearized elasticity theory, initial stresses, longitudinal wave; transverse wave; wave velocity

1 Introduction

The past two decades have seen the rapid growth of microelectromechanical systems (MEMS) that combine mechanical and electrical function in devices at very small scales, as an important area of technology [Ljung, Bachtold, Spasojevic

¹ Corresponding author. E-mail: m.kashtalyan@abdn.ac.uk, tel/fax: +44-1224-272519.

² Centre for Micro- and Nanomechanics (CEMINACS), School of Engineering, University of Aberdeen, Aberdeen, AB24 3UE, Scotland.

³ Timoshenko Institute of Mechanics, 3, Nesterov str., Kiev 03057, Ukraine.

(2000); Romanowicz, Zaman, Bart, Rabinovich, Tchertkov, Zhang, da Silva, Deshpande, Greiner, Gilbert, Cunningham (2000); Ye, Mukherjee (2000); Bettini, Brusa, Munteanu, Specogna Trevisan (2008)]. Examples of MEMS include pressure sensors, accelerometers, gyroscopes and optical devices, as well as chemical, biomedical and fluidic applications. The ability to integrate the mechanical (or biological or chemical) function with the electrical required for control and power conditioning in a single device allows for consideration of concepts such as the highly distributed networks required for health monitoring of large structures and systems or for distributed power and chemical production schemes.

Since MEMS typically contain several deposited and bonded layers of dissimilar materials, residual stresses can play an important role in determining their performance and reliability. Residual stresses in thin films and other deposited layers arise from several sources: thermal expansion mismatch, incorporation of residual gases into deposited materials, lattice mismatch, grain growth and grain size, sintering and the change in volume associated with incorporation or removal of defects. The relative importance of these stress producing mechanisms depends crucially on the materials, processing conditions and microstructure [Spearing (2000)]. Creation of MEMS devices with larger mechanical power and force capabilities may require deposition of thicker layers than those typically utilised in microelectronic applications. These thicker layers have a greater tendency to fracture and the thickness (and therefore size of the device that can be realised) may be limited by the residual stress state. The ability to control and characterize residual stresses is very important for the development of higher performance MEMS [Spearing (2000)].

Using adhesives in MEMS has not been very popular until recently due to chemical instability and remarkable changes of mechanical properties of adhesives during the life cycle. But with development of advanced dispersing techniques and improvement of properties of adhesives in general, they are starting to play a more important role in the field of microbonding [Niklaus, Enoksson, Kalvesten, Stemmes (2001); Satyanarayana, Karnik, Majumdar (2005); Kim, Kim, Hwang, Baek, Kim (2006); Andrijasevic, Smetana, Esinenco, Brenners (2006); Pang, Zhao, Du, Fang (2008)]. Adhesive microbonding can overcome some of drawbacks of the conventional microbonding, which is associated with demanding process requirements (high voltage, high process temperature, specific materials to be used, quality of surface, etc) which can restrain or disable the assembly process. Some advantages of adhesive microbonding are its lower process temperature; multi-material applicability; partial recyclability and possible biocompatibility. Additionally, it can be performed on all levels of package integration. Several different polymers can be used for adhesive bonding in MEMS, e.g. polyimides and epoxies. The choice of the polymer material used as an adhesive depends very much on the thermal,

chemical and mechanical requirements of the application.

To the best of our knowledge, residual stresses in adhesively bonded MEMS have been the subject of a very small number of studies in the literature. The effect of the stresses on the mechanical behaviour of such structures is little understood. Elastic deformation of adhesively bonded MEMS components taking into account residual stresses has been studied in [Sadaba, Fox, McWilliam (2006)] using a finite element model.

This paper investigates the effect of residual stresses on propagation of longitudinal and transverse waves along the layers in adhesively bonded multilayered structures for MEMS applications. The investigation is focused on the mechanical aspect of the problem. Therefore neither electric nor magnetic effects are taken into consideration. A multilayered structure analysed in the paper is assumed to be composed of infinite amount of the periodically recurring layers made of two different materials possessing significantly dissimilar properties: electrically conductive metal layer and insulating adhesive layer. The materials of both layers are assumed to be nonlinear elastic under the studied loading, and the elastic Murnaghan potential depending on the three invariants of strain tensor is used to describe their mechanical behaviour.

Propagation of the stationary plane waves with different polarization demands the three-dimensional problem statement to be used. The problem is formulated in the framework of the three-dimensional linearized elasticity theory of finite initial deformations. The dependencies of normalized velocity of the wave on two components of residual stresses in each layer as well as on the ratio of the layer thicknesses are examined and discussed.

2 Problem formulation

Stationary plane wave propagation in solids has been the subject of numerous studies in the literature, most recently [Menshykova, Menshykov, Guz (2009); Chakraborty (2009); Lee, Chen (2009); Wei, Su (2009); Guz, Menshykov, Zozulya, Guz (2007)]. Propagation of elastic waves in periodically layered macro, meso-, and microcomposites without and with residual stresses was studied in [Brekhovskikh (1960); Han (1977)] and [Guz (2002); Guz (2004); Guz, Zhuk, Makhort (1976); Guz, Han (1976)], respectively. Here, we formulate and solve the problem of propagation of the stationary plane elastic waves in a multilayered structure with periodically recurring layers for MEMS applications taking into account the presence of residual stresses. For this purpose, we employ the three-dimensional linearized theory of elasticity assuming that the initial strains are finite [Guz (2002); Guz (1999)]. Such approach appears to be highly suitable for analysis of multilayered

structures because it allows us to extend the description of material behaviour to situations where deviations from classical linear elasticity theory are noticeable. In [Zhuk, Guz (2006); Zhuk, Guz (2007)], this approach was used to study the propagation of a plane acoustic wave at a right angle to the layers of a laminated nanocomposite. Here we use it to analyze the propagation of plane waves along layers of a pre-stressed multilayered MEMS structure.

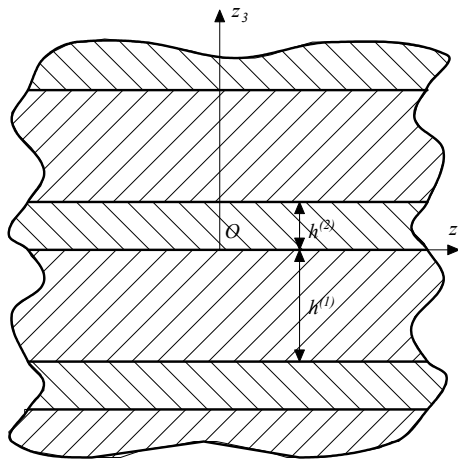


Figure 1: Multilayered structure

Using the approach developed in [Guz (2002); Guz (2004); Guz, Zhuk, Makhort (1976)] to study the propagation of plane elastic waves, we consider a multilayer structure consisting of two periodically recurring layers (see Fig. 1) – layer 1 being a conductive material and layer 2 a bonding adhesive material – with known densities ρ , Young moduli E , Poisson's ratios ν , as well as elastic moduli of the third order (Murnaghan constants) A , B , and C . Henceforth, all quantities associated with these layers will be denoted by corresponding numbers in parentheses. The materials of both conductive and adhesive layers are assumed to be compressible and isotropic.

As in [Guz (2002; Guz (2004))], we distinguish three states: (i) natural state (no stresses and strains in all layers); (ii) initial state labelled by the superscript "0"; and (iii) perturbed state (the superposition of the initial state and the stationary plane waves). It is also assumed that the stress amplitudes caused by the waves are much smaller than the stresses in the initial state. Such assumptions allow us to apply the three-dimensional linearized theory of elasticity [Guz (2002); Guz (1999)]. Indeed,

if all non-zero stresses in the initial state are much greater than the perturbations, then the equations of motion, strain-stress relations (equation of state), and boundary and initial conditions can be linearized with respect to this state. Henceforth, the term “linearized equations” will refer to equations for perturbations.

We will use the notation adopted in finite-strain theory and the most general elastic equations [Guz (2002); Guz (1999)]. Let us introduce two coordinate systems: (i) Lagrangian frame of reference (x_1, x_2, x_3) coinciding with the Cartesian coordinate system of the natural state and (ii) Cartesian coordinate system (z_1, z_2, z_3) of the initial state. It is obvious that Lagrangian frame of reference for the two neighbouring layers can differ in general case. Let the Cartesian coordinate system of the initial state be common for all layers (Fig. 1). This choice allows convenient analysis of the problem when the elongations of the materials are different.

The kinematic pattern of deformation is described by displacement fields $\vec{u}^{(j)}$, $(u_m^{(j)} = u_m^{(j)}(x_1, x_2, x_3, t))$, $j = 1, 2$; $m = 1, 2, 3$; t is time.

Denote the components of the Green strain tensor by ε_{mn} , $n = 1, 2, 3$. Then the elongations of infinitesimal elements directed, before deformation, along the unit vectors of the Cartesian coordinate system of the natural state are expressed as

$$\lambda_m = \sqrt{1 + 2\varepsilon_{mm}}, \quad m = 1, 2, 3,$$

where there is no summation over m on the right-hand side according to the indexing rules. For homogeneous initial states, we have

$$\begin{aligned} z_m &= \lambda_m^{(1)} x_m^{(1)}, \quad z_m = \lambda_m^{(2)} x_m^{(2)}, \quad \lambda_m^{(j)} = \text{const}, \quad j = 1, 2 \\ z_m &= x_m^{(j)} + u_m^{0(j)}, \quad u_m^{0(j)} = \delta_{mn} (\lambda_m^{(j)} - 1) x_n^{(j)}, \quad m, n = 1, 2, 3, \end{aligned} \quad (1)$$

where δ_{ij} is the Kronecker delta.

We assume that the mechanical behaviour of both materials is nonlinear elastic and can be described with the help of the elastic Murnaghan potential depending on the three invariants of strain tensor [Guz (2002); Guz (1999)]:

$$\Phi = \frac{1}{2} \lambda (A_1)^2 + \mu A_2 + \frac{A}{3} (A_1)^3 + B A_1 A_2 + \frac{C}{3} A_3. \quad (2)$$

where λ and μ are Lamé constants (elastic moduli of the second order)

$$\lambda = \frac{\nu E}{(1 + \nu)(1 - 2\nu)}, \quad \mu = \frac{E}{2(1 + \nu)}$$

and A_1 , A_2 , and A_3 are the first, second, and third algebraic invariants of the Green strain tensor ε_{ij} , which for a symmetric tensor of the second rank are determined

from the following formulas [Guz (2002); Guz (1999)]:

$$A_1 = \varepsilon_{ii}, \quad A_2 = \varepsilon_{ij}\varepsilon_{ji}, \quad A_3 = \varepsilon_{ij}\varepsilon_{jk}\varepsilon_{ki}, \quad i, j, k = 1, 2, 3.$$

In view of Eq. (1), the generalized stresses are given by

$$\sigma_{im}^{*0(j)} = \text{const}, \quad j = 1, 2, \quad i, m = 1, 2, 3. \quad (3)$$

Let the Oz_3 -axis be normal to the interface between the layers (Fig. 1). The thicknesses $h^{(j)}$ of the layers in the natural state and the thicknesses $\tilde{h}^{(j)}$ of the layers in the initial state are related by

$$\tilde{h}^{(j)} = \lambda_3^{(j)} h^{(j)}. \quad (4)$$

In the general case, the linearized equations of state for a compressible solid can be represented as follows [Guz (2002); Guz (1999)]:

$$\sigma_{in}^* = \lambda_{in\alpha\beta} u_{\alpha,\beta}, \quad t_{im} = \omega_{im\alpha\beta} u_{\alpha,\beta}, \quad i, n, m, \alpha, \beta = 1, 2, 3, \quad (5)$$

where t_{im} is the Kirchhoff tensor; $\lambda_{in\alpha\beta}$ and $\omega_{im\alpha\beta}$ are the components of fourth-rank tensors.

In the three-dimensional linearized theory of elasticity, the equations of motion with no perturbation of body forces in Lagrangian coordinates for a compressible solid with a homogeneous initial state, given by Eqs. (1), (2), have the form [Guz (2002); Guz (1999)]:

$$L_{m\alpha}^{(j)} u_{\alpha}^{(j)} = 0, \quad L_{m\alpha}^{(j)} = \omega_{im\alpha\beta}^{(j)} \frac{\partial^2}{\partial x_i^{(j)} \partial x_{\beta}^{(j)}} - \rho^{(j)} \delta_{m\alpha} \frac{\partial^2}{\partial t^2}; \quad i, m, \alpha, \beta = 1, 2, 3, \quad (6)$$

The components of the interface load at $x_3^{(j)} = \text{const}$, referred to the body configuration at the natural state, take the form

$$P_m^{*(j)} = \omega_{3m\alpha\beta}^{(j)} \frac{\partial u_{\alpha}^{(j)}}{\partial x_{\beta}^{(j)}}, \quad \alpha, \beta, m = 1, 2, 3. \quad (7)$$

These expressions are needed to formulate continuity and periodicity conditions.

Since all layers are isotropic in the natural state, then, considering the results obtained in [Guz (2002); Guz (2004)] and taking into account condition, given by Eq. (1) instead of Eq. (3), we obtain

$$\sigma_{im}^{*0(j)} = \delta_{in} \sigma_{mn}^{*0(j)}, \quad i, m, n = 1, 2, 3. \quad (8)$$

In this case, the components of tensor $\omega^{(j)}$ take form

$$\omega_{im\alpha\beta}^{(j)} = \lambda_m^{(j)} \lambda_\alpha^{(j)} \left[\delta_{im} \delta_{\alpha\beta} a_{i\beta}^{(j)} + \delta_{i\alpha} \delta_{m\beta} (1 - \delta_{im}) \mu_{im}^{(j)} + \delta_{m\alpha} \delta_{i\beta} (1 - \delta_{im}) \mu_{\beta m}^{(j)} \right]^+ \\ \delta_{\alpha m} \delta_{i\beta} \sigma_{ii}^{*0(j)}, \quad i, m, \alpha, \beta = 1, 2, 3. \quad (9)$$

Formulas for $a_{i\beta}^{(j)}$ and $\mu_{im}^{(j)}$ for compressible bodies were derived in [Guz (2002); Guz (2004)]. They should only be indexed to indicate the layer being dealt with.

It seems more convenient to formulate all the expressions in the Cartesian coordinates of the initial state. In this case, according to Eq. (1), we would have a common coordinate system for the conductive and adhesive layers.

Taking into account Eq. (1), we re-arrange the governing equations to the Cartesian coordinate system (z_1, z_2, z_3) of the initial state. According to Eqs.(1) and (6), they take the following form for compressible solids [Guz (2002); Guz (1999)]:

$$\tilde{L}_{m\alpha}^{(j)} u_\alpha^{(j)} = 0, \quad \tilde{L}_{m\alpha}^{(j)} = \tilde{\omega}_{im\alpha\beta}^{(j)} \frac{\partial^2}{\partial z_i \partial z_\beta} - \tilde{\rho}^{(j)} \delta_{m\alpha} \frac{\partial^2}{\partial \tau^2}, \quad i, m, n = 1, 2, 3, \quad (10)$$

where

$$\tilde{\omega}_{im\alpha\beta}^{(j)} = \frac{\lambda_i^{(j)} \lambda_\beta^{(j)}}{\lambda_1^{(j)} \lambda_2^{(j)} \lambda_3^{(j)}} \omega_{im\alpha\beta}^{(j)}; \quad \tilde{\rho}^{(j)} = \frac{\rho^{(j)}}{\lambda_1^{(j)} \lambda_2^{(j)} \lambda_3^{(j)}}, \quad (11)$$

and $\tilde{\rho}^{(j)}$ is the density in the initial state.

Let us consider the components of the interface load at $z_3 = \text{const}$ referred to the body configuration at the natural state. According to Eqs. (1) and (6), we have

$$\tilde{P}_m^{(j)} = \tilde{\omega}_{3m\alpha\beta}^{(j)} \frac{\partial u_\alpha^{(j)}}{\partial z_\beta}; \quad \tilde{P}_m^{(j)} = \frac{1}{\lambda_1^{(j)} \lambda_2^{(j)}} P_m^{*(j)}, \\ m, \alpha, \beta = 1, 2, 3. \quad (12)$$

The formulas for tensor ω remain the same. If all layers are isotropic in the natural state, then the relations, given by Eqs. (8) and (9), remain valid. Note that the conductive layers have thicknesses $\tilde{h}^{(1)}$ and adhesive layers are of thickness $\tilde{h}^{(2)}$ in the initial strain state, with $\tilde{h}^{(1)} \gg \tilde{h}^{(2)}$. The continuity and periodicity conditions on the interfaces (Fig. 1) are

$$u_m^{(1)}(0) = u_m^{(2)}(0); \quad \tilde{P}_m^{(1)}(0) = \tilde{P}_m^{(2)}(0), \quad (13)$$

$$u_m^{(1)}(\tilde{h}^{(1)}) = u_m^{(2)}(\tilde{h}^{(2)}); \quad \tilde{P}_m^{(1)}(\tilde{h}^{(1)}) = \tilde{P}_m^{(2)}(-\tilde{h}^{(2)}). \quad (14)$$

Thus, the problem of propagation of small elastic perturbations caused by the stationary plane wave in a prestrained multilayered structure is reduced to the linearized equations of motion, Eq. (10), with the continuity and periodicity conditions, Eqs. (13) and (14).

3 Solution method

Let us consider a stationary plane wave with a phase normal $\vec{n} = \{n_1, n_2, n_3\}$. As indicated in the previous section, the wave velocity and the phase normal will be referred to the Cartesian coordinate system at the initial state (z_1, z_2, z_3) . According to [Guz (2002); Guz (2004); Guz, Makhort (2000)], the solution of Eq. (10) can be represented in the form

$$u_\alpha^{(j)} = \hat{u}_\alpha^{(j)}(z_3) \exp[i(kn_\gamma z_\gamma - \omega t)], \quad \alpha, \gamma = 1, 2, 3, \quad (15)$$

where k is the wave number.

Substituting this trial solution, Eq. (15) into Eqs. (10), we obtain a system of ordinary differential equations for the amplitudes $\hat{u}_\alpha^{(j)}(z_3)$:

$$\exp[i(-kn_\gamma z_\gamma)] \tilde{\omega}_{im\alpha\beta}^{(j)} \frac{\partial^2}{\partial z_i \partial z_\beta} \hat{u}_\alpha^{(j)}(z_3) \exp[i(kn_q z_q)] + \tilde{\rho}^{(j)} \omega^2 \hat{u}_m^{(j)}(z_3) = 0; \quad (16)$$

$$i, m, q, \alpha, \beta, \gamma = 1, 2, 3.$$

To determine the components of the interface forces at $z_3 = \text{const}$, we substitute Eq. (15) into Eq. (12):

$$\tilde{P}_m^{(j)} = \hat{P}_m^{(j)}(z_3) \exp[i(kn_\gamma z_\gamma - \omega t)], \quad m, q, \alpha, \beta, \gamma = 1, 2, 3; \quad (17)$$

$$\hat{P}_m^{(j)}(z_3) = \exp[i(-kn_q z_q)] \tilde{\omega}_{3m\beta}^{(j)} \frac{\partial}{\partial z_\beta} \hat{u}_\alpha^{(j)}(z_3) \exp[i(kn_\gamma z_\gamma)].$$

Let us examine in detail the continuity and periodicity conditions, Eq. (13) and Eq. (14). Suppose we consider a system consisting of two neighbouring layers of conductive and adhesive materials. Let the conductive layer occupy the domain $-\tilde{h}^{(1)} \leq z_3 \leq 0$ on the Oz_3 -axis and the adhesive layer is within the domain $0 \leq z_3 \leq \tilde{h}^{(2)}$ on the same axis (Fig. 1). We will use the superscripts (1) and (2) to refer to the former and latter layers, respectively. Then the continuity conditions, Eq. (13), at $z_3 = 0$ become

$$\hat{u}_m^{(1)}(0) = \hat{u}_m^{(2)}(0); \quad \hat{P}_m^{(1)}(0) = \hat{P}_m^{(2)}(0), \quad m = 1, 2, 3, \quad (18)$$

By virtue of the Floquet theorem [Brillouin, Parodi (1953)], the amplitudes $\hat{u}_m^{(j)}(z_3)$ and $\hat{P}_m^{(j)}(z_3)$ must satisfy the following periodicity conditions, which are similar to Eq. (14):

$$\hat{u}_m^{(1)}(\tilde{h}^{(1)}) = \hat{u}_m^{(2)}(\tilde{h}^{(2)}); \quad \hat{P}_m^{(1)}(\tilde{h}^{(1)}) = \hat{P}_m^{(2)}(-\tilde{h}^{(2)}), \quad m = 1, 2, 3. \quad (19)$$

Thus, it is necessary to solve a set of ordinary differential equations, Eqs. (16), i.e. to determine functions $u_\alpha^{(j)}(z_3)$, find the functions $\hat{P}_m^{(j)}(z_3)$ from the second relation in Eq. (17) and substitute the resulting expressions into the continuity and periodicity conditions, Eqs. (18) and (19). After that, a dispersion equation can be derived from the requirement that set of algebraic equations has a non-trivial solution.

4 Propagation of plane waves along layers

Let a sequence of manufacturing processes induce the residual stresses $\sigma_{33}^{*0(1)}$, $\sigma_{33}^{*0(2)}$, $\sigma_{11}^{*0(1)}$ and $\sigma_{11}^{*0(2)}$ in each layer of the multilayered structure. We assume that these stresses are homogeneous and, in the general case, different in dissimilar layers; the layers are relatively rigid (no large strains); and applied loads do not exceed the yield limit. Then, we can restrict ourselves to the first approximation of the linearized theory of elastic waves in pre-stressed solids. For this approximation, we will take the modification of the theory where the wave velocities are determined by neglecting the second order terms with respect to (P_j^0/μ) in the coefficients appearing in the equations of the problem. Here, μ is the shear modulus and P_j^0 is the intensity of the external load acting on the body in the initial stress-strain state and referred to the natural (undeformed) configuration of the body [Guz (2002); Guz (2004)]. Since materials are elastic, and the loads are small compared with the elastic limit, we can use true stresses instead of generalized stresses: $\sigma_{11}^{*0(j)} = \sigma_{11}^{0(j)}$, $\sigma_{33}^{*0(j)} = \sigma_{33}^{0(j)}$, $j = 1, 2$.

Let us now consider a plane acoustic wave propagating in the multilayered structure. Then the manufacturing residual stresses are considered as the initial ones in the problem of propagation of low-amplitude waves. We will examine the effect of these stresses on the macroscopic properties (in particular, the velocity of acoustic waves) of the multilayered structure for different ratios of the layers thickness.

We will examine in detail the following two cases: (a) waves are polarized in the plane z_1Oz_3 and (b) displacements of the body are parallel to the Oz_2 -axis.

4.1 Waves polarized in the plane $z_1 O z_3$

Let us consider waves polarized in the plane $z_1 O z_3$ ($u_2^{(j)} = 0$) that have the wave vector $\vec{k} = (k, 0, 0)$. According to [Han (1977); Guz, Han (1976)], the solution of Eq. (10) can be represented in the form

$$u_\alpha^{(j)} = \hat{u}_\alpha^{(j)} \exp [i (kz_1 - \omega t)], \hat{u}_3^{(j)} = A^{(j)} \exp [ia^{(j)} z_3], u_1^{(j)} = \gamma^{(j)} \hat{u}_3^{(j)}, \alpha = 1, 3, j = 1, 2, \quad (20)$$

where $A^{(j)}$, $a^{(j)}$ and $\gamma^{(j)}$ are some constants.

Following the procedure outlined in the previous section, we substitute Eq. (20) into Eq. (10) to obtain

$$\begin{aligned} \gamma^{(j)} \left(\tilde{\omega}_{1111}^{(j)} k^2 + \tilde{\omega}_{3113}^{(j)} a^{(j)2} - \tilde{\rho}^{(j)} \omega^2 \right) + \left(\tilde{\omega}_{1313}^{(j)} + \tilde{\omega}_{1133}^{(j)} \right) ka^{(j)} &= 0; \\ \gamma^{(j)} \left(\tilde{\omega}_{1313}^{(j)} + \tilde{\omega}_{1133}^{(j)} \right) ka^{(j)} + \left(\tilde{\omega}_{1331}^{(j)} k^2 + \tilde{\omega}_{3333}^{(j)} a^{(j)2} - \tilde{\rho}^{(j)} \omega^2 \right) &= 0. \end{aligned} \quad (21)$$

Equations (21) yield four solutions for $a^{(j)}$: $a_1^{(j)} = -a_2^{(j)}$; $a_3^{(j)} = -a_4^{(j)}$. Then the representation, given by Eq. (20), becomes

$$\begin{aligned} \hat{u}_3^{(j)} &= A_1^{(j)} \exp (ia_1^{(j)} z_3) + A_2^{(j)} \exp (-ia_1^{(j)} z_3) + A_3^{(j)} \exp (ia_3^{(j)} z_3) \\ &\quad + A_4^{(j)} \exp (-ia_3^{(j)} z_3); \\ \hat{u}_1^{(j)} &= \gamma_1^{(j)} \left[A_1^{(j)} \exp (ia_1^{(j)} z_3) - A_2^{(j)} \exp (-ia_1^{(j)} z_3) \right] + \\ &\quad \gamma_3^{(j)} \left[A_3^{(j)} \exp (ia_3^{(j)} z_3) - A_4^{(j)} \exp (-ia_3^{(j)} z_3) \right]. \end{aligned} \quad (22)$$

Considering two neighbouring layers, we take continuity and periodicity conditions at $z_3 = \text{const}$ in the form of Eq. (18) and Eq. (19), respectively, with the only difference that the index m takes the values 1 and 3. These conditions yield a homogeneous system of algebraic equations of the eighth order, omitted here for the sake of brevity. A requirement for this set of equations to have a non-trivial solution leads to the dispersion equation.

Let us apply this procedure to some special types of waves.

4.1.1 Quasi-shear waves

Let $u_1^{(j)}$ be asymmetric (odd) and $u_3^{(j)}$ be symmetric (even) about the middle surfaces of the layers. This type of motion is schematically shown in Fig. 2a. Such

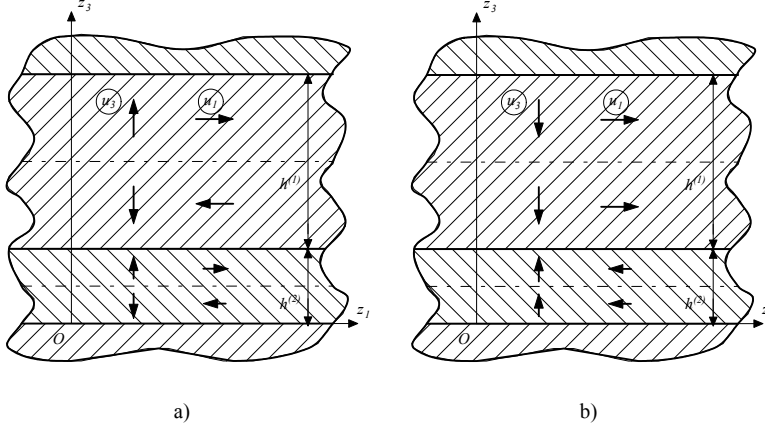


Figure 2: Schematic representation of: a) quasi-shear wave and b) quasi-compressional wave

a wave within each layer is referred to as *quasi-shear* [Guz (2004)] or *shear in the mean* [Brekhovskikh (1960); Behrens (1967)].

Let us consider waves polarized in the plane z_1Oz_3 ($u_2^{(j)} = 0$) that have the wave vector $\vec{k} = (k, 0, 0)$. According to [Han (1977), Guz, Han (1976)], the solution of Eq. (10) can be represented in the form of Eq. (20). Then Eqs. (22) become

$$\begin{aligned}
 \hat{u}_1^{(1)} &= \gamma_1^{(1)} \left\{ \bar{A}_1^{(1)} \exp \left[ia_1^{(1)} \left(z_3 - \tilde{h}^{(1)}/2 \right) \right] - \bar{A}_2^{(1)} \exp \left[-ia_1^{(1)} \left(z_3 - \tilde{h}^{(1)}/2 \right) \right] \right\} + \\
 &\quad \gamma_3^{(1)} \left\{ \bar{A}_3^{(1)} \exp \left[ia_3^{(1)} \left(z_3 - \tilde{h}^{(1)}/2 \right) \right] - \bar{A}_4^{(1)} \exp \left[-ia_3^{(1)} \left(z_3 - \tilde{h}^{(1)}/2 \right) \right] \right\}; \\
 \hat{u}_1^{(2)} &= \gamma_1^{(2)} \left\{ \bar{A}_1^{(2)} \exp \left[ia_1^{(2)} \left(z_3 + \tilde{h}^{(2)}/2 \right) \right] - \bar{A}_2^{(2)} \exp \left[-ia_1^{(2)} \left(z_3 + \tilde{h}^{(2)}/2 \right) \right] \right\} + \\
 &\quad \gamma_3^{(2)} \left\{ \bar{A}_3^{(2)} \exp \left[ia_3^{(2)} \left(z_3 + \tilde{h}^{(2)}/2 \right) \right] - \bar{A}_4^{(2)} \exp \left[-ia_3^{(2)} \left(z_3 + \tilde{h}^{(2)}/2 \right) \right] \right\};.
 \end{aligned} \tag{23}$$

The relations for $\hat{u}_3^{(1)}$ and $\hat{u}_3^{(2)}$ can be written in a similar manner.

For the wave in question, $\bar{A}_1^{(j)} = \bar{A}_2^{(j)}$, $\bar{A}_3^{(j)} = \bar{A}_4^{(j)}$ and, hence, the continuity and periodicity conditions in terms of amplitudes, Eq. (18) and Eq. (19) coincide. Therefore, one can obtain a homogeneous system of four algebraic equations for $\bar{A}_1^{(j)}$ and $\bar{A}_3^{(j)} = \bar{A}_4^{(j)}$. Equating the determinant of this system to zero, we arrive at the dispersion equation derived in [Han (1977)].

This equation is essentially nonlinear and very complicated in structure, and also extremely difficult to solve. However, using the long-wave approximation, which

is of special interest for the class of problems and objects considered here, can significantly simplify this equation. In this case, in view of Eq. (21), the dispersion equation yields an expression for the squared velocity of a quasi-shear wave polarized in the plane z_1Oz_3 and propagating along the Oz_1 -axis in the presence of initial stresses

$$c_{z_1z_3}^2 = \frac{\tilde{\omega}_{1331}^{(1)} \tilde{h}^{(1)} + \tilde{\omega}_{1331}^{(2)} \tilde{h}^{(2)} - [\tilde{\omega}_{3113}^{(2)} \tilde{h}^{(1)} + \tilde{\omega}_{3113}^{(1)} \tilde{h}^{(2)}]^{-1} \tilde{h}^{(1)} \tilde{h}^{(2)} (\tilde{\omega}_{1313}^{(1)} - \tilde{\omega}_{1313}^{(2)})^2}{\tilde{\rho}^{(1)} \tilde{h}^{(1)} + \tilde{\rho}^{(2)} \tilde{h}^{(2)}}, \quad (24)$$

where the first subscript indicates the direction of wave propagation and the second subscript notes the preferred (in the mean) direction of displacements in the medium. Let us introduce the ratio of the layers thickness in the natural state as

$$q = h^{(2)} / h^{(1)}. \quad (25)$$

Taking into account Eqs. (1), (4), (9), and (25), we obtain

$$c_{z_1z_3}^2 = \left(\frac{\rho^{(1)}}{\lambda_1^{(1)} \lambda_2^{(1)}} + \frac{q\rho^{(2)}}{\lambda_1^{(2)} \lambda_2^{(2)}} \right)^{-1} \left[\frac{\lambda_1^{(1)}}{\lambda_2^{(1)}} \left(\lambda_3^{(1)2} \mu_{13}^{(1)} + \sigma_{11}^{0(1)} \right) + \frac{q\lambda_1^{(2)}}{\lambda_2^{(2)}} \left(\lambda_3^{(2)2} \mu_{13}^{(2)} + \sigma_{11}^{0(2)} \right) - \left(\frac{\lambda_1^{(1)} \lambda_3^{(1)} \mu_{13}^{(1)}}{\lambda_2^{(1)}} - \frac{\lambda_1^{(2)} \lambda_3^{(2)} \mu_{13}^{(2)}}{\lambda_2^{(2)}} \right)^2 \left(\frac{\lambda_1^{(2)2} \mu_{13}^{(2)} + \sigma_{33}^{0(2)}}{q\lambda_1^{(2)} \lambda_2^{(2)}} + \frac{\lambda_1^{(1)2} \mu_{13}^{(1)} + \sigma_{33}^{0(1)}}{\lambda_1^{(1)} \lambda_2^{(1)}} \right)^{-1} \right]. \quad (26)$$

Let us denote the velocity of a wave in a multilayered structure without initial stresses by $v_{x_1x_3}$, where the subscripts x_1 and x_3 indicate that the velocity is a macroscopic property of the composite referred to the coordinate system of the natural state. Equating the initial strains in Eq. (26) to zero and using the elastic potential of a linear elastic body, we arrive at the following relation for $v_{x_1x_3}$:

$$v_{x_1x_3}^2 = \frac{\mu^{(1)} + q\mu^{(2)} - [\mu^{(2)} + q\mu^{(1)}]^{-1} q (\mu^{(1)} - \mu^{(2)})^2}{\rho^{(1)} + q\rho^{(2)}} \quad (27)$$

To characterize the effect of residual stresses, we will estimate the relative velocity η_{13} of a plane wave as

$$\eta_{13} = \frac{c_{z_1 z_3} - v_{x_1 x_3}}{v_{x_1 x_3}}. \quad (28)$$

It follows from Eq. (26) that $\lambda_1^{(j)}$, $\lambda_2^{(j)}$, $\lambda_3^{(j)}$ and $\mu_{13}^{(j)}$ should be calculated to make use of Eq. (28). Using the general results obtained in [Guz (2004)],

$$\mu_{i\beta}^{(j)} = \mu^{(j)} + \frac{B^{(j)} \sigma_{\alpha\alpha}^{0(j)}}{3K_0^{(j)}} + \frac{C^{(j)}}{4\mu^{(j)}} \left[\left(\sigma_{ii}^{0(j)} + \sigma_{\beta\beta}^{0(j)} \right) - \frac{2\lambda^{(j)} \sigma_{\alpha\alpha}^{0(j)}}{3K_0^{(j)}} \right], \quad (29)$$

(no summation over doubled i and β in Eq. (29)), we arrive at the expressions

$$\begin{aligned} \lambda_1^{(j)2} &= 1 + \frac{2(\lambda^{(j)} + \mu^{(j)}) \sigma_{11}^{0(j)} - \lambda^{(j)} \sigma_{33}^{0(j)}}{3K_0^{(j)} \mu^{(j)}}, & \lambda_2^{(j)2} &= 1 - \frac{\lambda^{(j)} (\sigma_{11}^{0(j)} + \sigma_{33}^{0(j)})}{3K_0^{(j)} \mu^{(j)}}, \\ \lambda_3^{(j)2} &= 1 + \frac{2(\lambda^{(j)} + \mu^{(j)}) \sigma_{33}^{0(j)} - \lambda^{(j)} \sigma_{11}^{0(j)}}{3K_0^{(j)} \mu^{(j)}}, \\ \mu_{13}^{(j)} &= \mu^{(j)} \left[1 + \frac{(\sigma_{11}^{0(j)} + \sigma_{33}^{0(j)})}{3K_0^{(j)} \mu^{(j)}} \left(B^{(j)} + \frac{\lambda^{(j)} + 2\mu^{(j)}}{4\mu^{(j)}} C^{(j)} \right) \right]. \end{aligned} \quad (30)$$

These formulas allow us to determine the relative velocity of a plane wave and to examine the influence of the residual stresses and the ratio of the layers thickness on the wave propagation pattern.

4.1.2 Quasi-compressional waves

Suppose that $\sigma_{11}^{0(j)} \neq 0$, $\sigma_{33}^{0(j)} \neq 0$, and $\sigma_{22}^{0(j)} = 0$, $j = 1, 2$. Let $u_1^{(j)}$ be symmetric (even) and $u_3^{(j)}$ be asymmetric (odd) about the middles of the layers. This type of motion is schematically shown in Fig. 2b. Such a wave within each layer is referred to as *quasi-compressional* [Guz (2004)] or *compressional in the mean* [Brekhovskikh (1960); Behrens (1967)]. Here it is necessary to set $\bar{A}_1^{(j)} = -\bar{A}_2^{(j)}$, $\bar{A}_3^{(j)} = -\bar{A}_4^{(j)}$ in Eq. (23).

Following the procedure outlined in subsection 4.1.1, we obtain, from Eqs. (18) and (19), a homogeneous system of equations for $\bar{A}_1^{(j)}$ and $\bar{A}_3^{(j)}$. Equating its determinant to zero, we arrive at a dispersion equation in a quite complicated form [Han (1977)].

The equation can be simplified significantly by using the long-wave approximation. In view of Eq. (21), the dispersion equation yields the squared velocity of a quasi-compressional wave polarized in the plane z_1Oz_3 and propagating along the Oz_1 -axis in the presence of initial stresses as

$$c_{z_1z_1}^2 = \frac{\tilde{\omega}_{1111}^{(1)} \tilde{h}^{(1)} + \tilde{\omega}_{1111}^{(2)} \tilde{h}^{(2)} - \left[\tilde{\omega}_{3333}^{(2)} \tilde{h}^{(1)} + \tilde{\omega}_{3333}^{(1)} \tilde{h}^{(2)} \right]^{-1} \tilde{h}^{(1)} \tilde{h}^{(2)} \left(\tilde{\omega}_{1133}^{(1)} - \tilde{\omega}_{1133}^{(2)} \right)^2}{\tilde{\rho}^{(1)} \tilde{h}^{(1)} + \tilde{\rho}^{(2)} \tilde{h}^{(2)}}. \quad (31)$$

Taking (1), (4), (9), and (25) into account, we get

$$c_{z_1z_1}^2 = \left(\frac{\rho^{(1)}}{\lambda_1^{(1)} \lambda_2^{(1)}} + \frac{q\rho^{(2)}}{\lambda_1^{(2)} \lambda_2^{(2)}} \right)^{-1} \left[\frac{\lambda_1^{(1)}}{\lambda_2^{(1)}} \left(\lambda_1^{(1)2} a_{11}^{(1)} + \sigma_{11}^{0(1)} \right) + \frac{q\lambda_1^{(2)}}{\lambda_2^{(2)}} \left(\lambda_1^{(2)2} a_{11}^{(2)} + \sigma_{11}^{0(2)} \right) - \left(\frac{\lambda_1^{(1)} \lambda_3^{(1)} a_{13}^{(1)}}{\lambda_2^{(1)}} - \frac{\lambda_1^{(2)} \lambda_3^{(2)} a_{13}^{(2)}}{\lambda_2^{(2)}} \right)^2 \left(\frac{\lambda_3^{(2)2} a_{33}^{(2)} + \sigma_{33}^{0(2)}}{q\lambda_1^{(2)} \lambda_2^{(2)}} + \frac{\lambda_3^{(1)2} a_{33}^{(1)} + \sigma_{33}^{0(1)}}{\lambda_1^{(1)} \lambda_2^{(1)}} \right)^{-1} \right]. \quad (32)$$

Let us denote the velocity of a quasi-compressional wave in a multilayered structure without residual stresses by $v_{x_1x_1}$. The meaning of the subscripts is the same as in subsection 4.1.1. Equating the initial strains in Eq. (32) to zero and using the elastic potential of a linear elastic body, we arrive at the following expression for $v_{x_1x_1}$:

$$v_{x_1x_1}^2 = \frac{\left(\frac{(\lambda^{(1)} + 2\mu^{(1)}) + q(\lambda^{(2)} + 2\mu^{(2)}) - [(\lambda^{(2)} + 2\mu^{(2)}) + q(\lambda^{(1)} + 2\mu^{(1)})]^{-1} q(\lambda^{(1)} - \lambda^{(2)})^2}{\rho^{(1)} + q\rho^{(2)}} \right)}{\rho^{(1)} + q\rho^{(2)}} \quad (33)$$

To characterize the effect of residual stresses, we will estimate the relative velocity η_{11} of a plane wave:

$$\eta_{11} = \frac{c_{z_1z_1} - v_{x_1x_1}}{v_{x_1x_1}}. \quad (34)$$

It follows from Eq. (32) that $\lambda_1^{(j)}$, $\lambda_2^{(j)}$, $\lambda_3^{(j)}$, $a_{11}^{(j)}$, $a_{13}^{(j)}$ and $a_{33}^{(j)}$ should be calculated to make use of Eq. (34). The first three quantities can be determined from the

first three formulas in Eq. (30). To determine $a_{11}^{(j)}$, $a_{13}^{(j)}$ and $a_{33}^{(j)}$, we use the results obtained in [Guz (2002); Guz (2004)]. For example, the following general relation for $a_{i\beta}^{(j)}$ has been derived in [Guz (2004)]:

$$a_{i\beta}^{(j)} = \lambda^{(j)} + \frac{B^{(j)}}{\mu^{(j)}} \left(\sigma_{ii}^{0(j)} + \sigma_{\beta\beta}^{0(j)} \right) + \frac{2}{3K_0^{(j)}} \left(a^{(j)} - \frac{B^{(j)}\lambda^{(j)}}{\mu^{(j)}} \right) \sigma_{\alpha\alpha}^{0(j)} + 2\delta_{i\beta} \left[\mu^{(j)} + \frac{C^{(j)}\sigma_{ii}^{0(j)}}{2\mu^{(j)}} + \frac{\sigma_{\alpha\alpha}^{0(j)}}{3K_0^{(j)}} \left(B^{(j)} - \frac{C^{(j)}\lambda^{(j)}}{2\mu^{(j)}} \right) \right]. \quad (35)$$

Here there is no summation over doubled i and β , as in Eq. (29).

Thus, we arrive at the expressions

$$a_{11}^{(j)} = \left(\lambda^{(j)} + 2\mu^{(j)} \right) \left[1 + \frac{\left(\sigma_{11}^{0(j)} + \sigma_{33}^{0(j)} \right) \left(2A^{(j)}\mu^{(j)} - 2B^{(j)} \left(\lambda^{(j)} - \mu^{(j)} \right) - \lambda^{(j)}C^{(j)} \right)}{3K_0^{(j)}\mu^{(j)} \left(\lambda^{(j)} + 2\mu^{(j)} \right)} + \frac{\sigma_{11}^{0(j)} \left(2B^{(j)} + C^{(j)} \right)}{\mu^{(j)} \left(\lambda^{(j)} + 2\mu^{(j)} \right)} \right], \quad (36)$$

$$a_{13}^{(j)} = \lambda^{(j)} + \frac{\left(\sigma_{11}^{0(j)} + \sigma_{33}^{0(j)} \right)}{3K_0^{(j)}} \left(2a^{(j)} + \frac{B^{(j)} \left(\lambda^{(j)} + 2\mu^{(j)} \right)}{\mu^{(j)}} \right),$$

$$a_{33}^{(j)} = \left(\lambda^{(j)} + 2\mu^{(j)} \right) \left[1 + \frac{\left(\sigma_{11}^{0(j)} + \sigma_{33}^{0(j)} \right) \left(2A^{(j)}\mu^{(j)} - 2B^{(j)} \left(\lambda^{(j)} - \mu^{(j)} \right) - \lambda^{(j)}C^{(j)} \right)}{3K_0^{(j)}\mu^{(j)} \left(\lambda^{(j)} + 2\mu^{(j)} \right)} + \frac{\sigma_{33}^{0(j)} \left(2B^{(j)} + C^{(j)} \right)}{\mu^{(j)} \left(\lambda^{(j)} + 2\mu^{(j)} \right)} \right].$$

The above expressions, Eq. (36), allow us to determine the relative velocity of a longitudinal plane wave, Eq. (34), propagating along the Oz_1 -axis if the moduli of the second and third order of the layers are known. By changing the magnitude and type of residual stresses and the thickness ratio of the layers, we can study their influence on the behaviour of quasi-compressional waves. This is useful for the determining the residual stresses and identifying the internal pattern of the multi-layered structure.

4.2 Purely shear waves

Let us consider a purely shear wave propagating along the Oz_1 -axis. In this case, only the

displacement components $u_2^{(j)}$ are nonzero:

$$u_2^{(j)} \neq 0, \quad u_1^{(j)} = u_3^{(j)} = 0.$$

Then, according to [Han (1977); Guz (2002)], the solution is sought in the form

$$u_2^{(j)} = a^{(j)} \exp\left(ia^{(j)}z_3\right) \exp[i(kz_1 - \omega t)]. \quad (37)$$

Substituting Eq. (37) into Eq. (10), we obtain

$$a^{(j)2} = -\tilde{\omega}_{3223}^{(j)-1} \left(\tilde{\omega}_{1221}^{(j)} k^2 - \tilde{\rho}^{(j)} \omega^2 \right).$$

The displacement $u_2^{(j)}$ can be expressed as

$$u_2^{(j)} = \left(A_1^{(j)} \exp\left[ia^{(j)}z_3\right] + A_2^{(j)} \exp\left[-ia^{(j)}z_3\right] \right) \exp[i(kz_1 - \omega t)]. \quad (38)$$

Substituting Eq. (38) into Eq. (18) and Eq. (19), we arrive at the following dispersion equation [Han (1977)]

$$\begin{aligned} & 2\tilde{\omega}_{3223}^{(1)} \tilde{\omega}_{3223}^{(2)} a^{(1)} a^{(2)} \left(1 - \cos a^{(1)} \tilde{h}^{(1)} \cos a^{(2)} \tilde{h}^{(2)} \right) + \\ & \left(\tilde{\omega}_{3223}^{(1)} a^{(1)2} + \tilde{\omega}_{3223}^{(2)} a^{(2)2} \right) \sin a^{(1)} \tilde{h}^{(1)} \sin a^{(2)} \tilde{h}^{(2)} = 0. \end{aligned} \quad (39)$$

Using the long-length approximation, used previously in subsections 4.1.1 and 4.1.2, we obtain the velocity of a shear wave in a multilayered structure as

$$\begin{aligned} c_{z_1 z_2}^2 = & \left(\frac{\rho^{(1)}}{\lambda_1^{(1)} \lambda_2^{(1)}} + \frac{q\rho^{(2)}}{\lambda_1^{(2)} \lambda_2^{(2)}} \right)^{-1} \\ & \left[\frac{\lambda_1^{(1)}}{\lambda_2^{(1)}} \left(\lambda_2^{(1)2} \mu_{12}^{(1)} + \sigma_{11}^{0(1)} \right) + \frac{q\lambda_1^{(2)}}{\lambda_2^{(2)}} \left(\lambda_1^{(2)2} \mu_{12}^{(2)} + \sigma_{11}^{0(2)} \right) \right]. \end{aligned} \quad (40)$$

In the absence of residual stresses, this velocity is given by

$$v_{x_1 x_2}^2 = \frac{\mu^{(1)} + q\mu^{(2)}}{\rho^{(1)} + q\rho^{(2)}}. \quad (41)$$

To examine the effect of the initial stresses and thickness ratio, we will consider the relative velocity η_{12} of a plane wave

$$\eta_{12} = \frac{c_{z_1 z_2} - v_{x_1 x_2}}{v_{x_1 x_2}}. \quad (42)$$

All quantities in Eq. (40), except for $\mu_{12}^{(j)}$, are known. To determine this coefficient, we again take advantage of Eq. (29)

$$\mu_{12}^{(j)} = \mu^{(j)} + \frac{\sigma_{11}^{0(j)} + \sigma_{33}^{0(j)}}{3K_0^{(j)}} + \frac{C^{(j)}}{4\mu^{(j)}} \left[\sigma_{11}^{0(j)} - \frac{2\lambda^{(j)}}{3K_0^{(j)}} (\sigma_{11}^{0(j)} + \sigma_{33}^{0(j)}) \right]. \quad (43)$$

These formulas allow us to determine the relative velocity, Eq. (42), of a plane wave and to examine the effect of the initial stresses and thickness ratio on the propagation pattern of purely shear waves.

5 Results and discussion

Let us consider plane waves propagating in a multilayered structure consisting of periodically recurring electrically conductive (metal) and adhesive (plastic) layers modelled by isotropic materials described by a Murnaghan-type potential, Eq. (2). To this end, we will analyze the dependence of Eqs. (28), (34), and (42) on the residual stresses and on the thickness ratio of the layers, q .

To assess the method developed here, we use the following model materials: polystyrene (PS), a 90:10 mixture of EPON-828 epoxy resin and polystyrene (EP-PS), polymethyl methacrylate (PMMA), steel, bronze, and brass, with properties listed in Table 1. Nine compositions can be made up of these materials. For brevity, we denote them by the letter C followed by a sequence number. The possible compositions are summarized in Table 2 and arranged into three groups: I (C1, C2, C3), II (C4, C5, C6), and III (C7, C8, C9), depending on the type of the softer material.

To facilitate analysis, results will be presented in terms of $\psi_1^{(j)}$ and $\psi_3^{(j)}$, where $\psi_1^{(j)} = \sigma_{11}^{0(j)} / \mu^{(1)}$, $\psi_3^{(j)} = \sigma_{33}^{0(j)} / \mu^{(1)}$, $j = 1, 2$, i.e. residual stresses in a given layer will be normalised by the shear modulus of the stiffer material of the composition (metal), labelled with the superscript (1) (Fig. 1).

Analysis of the numerical results for all the compositions listed in Table 2 shows that the dependences of η on ψ and of η on q are qualitatively similar within each group. Therefore, we will only present the most typical results for each group.

The properties of the adhesive layer seem to be the major factor that governs the behaviour of the graphs for given levels of normalised residual stresses ($-5 \cdot 10^{-4} \leq$

Table 1: Density ρ , Lamé constants λ and μ (elastic moduli of the second order), and Murnaghan constants A , B , and C (elastic moduli of the third order) for the conductive and adhesive layer materials

Material	ρ , kg/m ³	λ , GPa	μ , GPa	A , GPa	B , GPa	C , GPa
PS	$1.050 \cdot 10^3$	1.71	1.140	-10.8	-7.85	-9.81
EP-PS	$1.195 \cdot 10^3$	3.424	0.977	-1.08	-0.785	-0.981
PMMA	$1.16 \cdot 10^3$	4.04	1.9	0.268	-3.12	-6.77
Steel	$7.795 \cdot 10^3$	92.6	77.5	-235.0	-275.0	-490.0
Brass	$7.20 \cdot 10^3$	94.9	44.7	-70.0	270.0	-340.0
Bronze	$7.20 \cdot 10^3$	81.6	38.4	120.0	-310.0	480.0

Table 2: Compositions investigated

Group	Composition	Composition
I	C1	Steel – PMMA
	C2	Brass – PMMA
	C3	Bronze – PMMA
II	C4	Steel – EP-PS
	C5	Brass – EP-PS
	C6	Bronze – EP-PS
III	C7	Steel – PS
	C8	Brass – PS
	C9	Bronze – PS

$\psi_i^{(j)} \leq 5 \cdot 10^{-4}$, $i = 1, 3$; $j = 1, 2$) and thickness ratio q ($0 \leq q \leq 0.5$). The solid, dash-and-dot, and dashed lines represent the parameters η_{13} , η_{12} , and η_{11} , respectively.

Figure 3 shows the relative velocities of plane waves propagating along the Oz_1 -axis as a function of the layer thickness ratio q in a steel-PS composition (C1 in Table 2) with $\psi_3^{(1)} = \psi_3^{(2)} = \psi_1^{(1)} = 0$, $\psi_1^{(2)} = 5 \cdot 10^{-4}$, i.e., when the residual stress $\sigma_{11}^{0(2)} = 38.75$ MPa and the other three residual stresses are zero. As can be seen, the parameters η_{12} monotonically increase with q . The rate of increase in the relative velocity is constant for the investigated interval of q . Thus, the longitudinal tensile stress induced in the softer adhesive layer increases the velocity of purely shear plane waves. The behaviour of the relative velocity η_{13} of quasi-shear plane wave is also monotonous but decreasing with the q increases. Also, η_{13} is negative unlike η_{12} . It quickly drops to the value of -0.3 approximately at the $q \approx 0.1$ and then slightly decreases as the q approaches the value of 0.5.

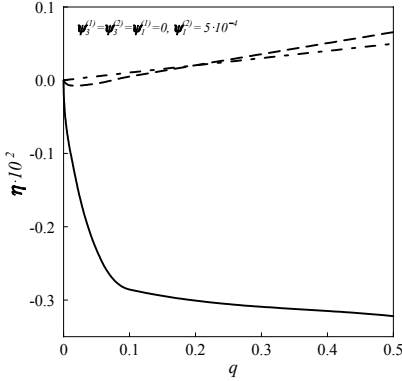


Figure 3: Normalized relative velocities of plane waves propagating along the Oz_1 -axis as a function of the thickness ratio of layers q in a multilayered structure with C1 composition

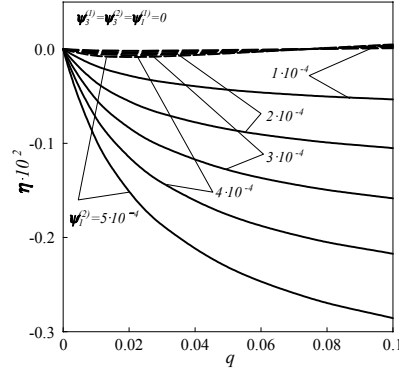


Figure 4: Normalized relative velocities η_{13} and η_{11} vs q for different levels of normalized residual stress $\psi_1^{(2)}$ for C1 composition (small q)

The behaviour of the velocity of a quasi-compressional wave is essentially different under these conditions. The parameter η_{11} is negative in the interval $0 < q \leq 0.9$ initially decreasing with increase in the layer thickness of PS, reaching a minimum of $\eta_{11} \approx -0.7 \cdot 10^{-2}$ at $q \approx 0.2 \cdot 10^{-1}$. Next, the relative velocity of the quasi-compressional wave increases and becomes equal to zero at $q \approx 0.75 \cdot 10^{-1}$. This means that there exists a thickness ratio of the layers such that the velocity of a quasi-compressional wave in a multilayered structure with residual stress $\sigma_{11}^{0(2)}$ in the PS layer is equal to its velocity in the corresponding composition without residual stresses.

Detailed analysis of this phenomenon for different levels of the residual stress $\sigma_{11}^{0(2)}$ is presented in Fig. 4, which shows the behaviour of η_{13} and η_{11} for small values of q . The values of $\psi_1^{(2)}$ are indicated near the curves. It can be seen that the effect persists. Moreover, when $q \approx 0.75 \cdot 10^{-1}$, the velocity of a quasi-compressional wave in a multilayered structure with any level of pre-stress is equal to its velocity in the corresponding structure without pre-stresses. Increase in $\psi_1^{(2)}$ leads to an increase in the absolute value of the local minimum of η_{12} as a function of q . Conversely, decrease in the residual stress causes the curve of the relative velocity versus the thickness ratio, as one would expect, to tend to the horizontal axis, which corresponds to a stress-free material.

Figure 5 shows the dependences of η_{12} and η_{13} on q for different values of $\psi_1^{(2)}$

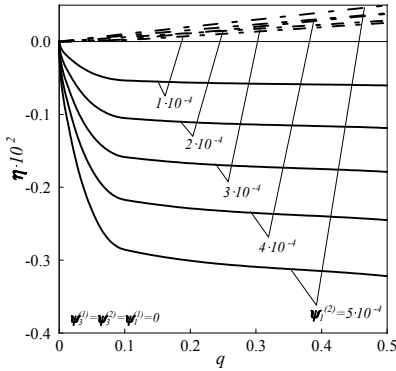


Figure 5: Effect of different levels of residual stresses $\sigma_{11}^{0(2)}$ on the relative velocities η_{13} and η_{12} dependences on q for C1 composition

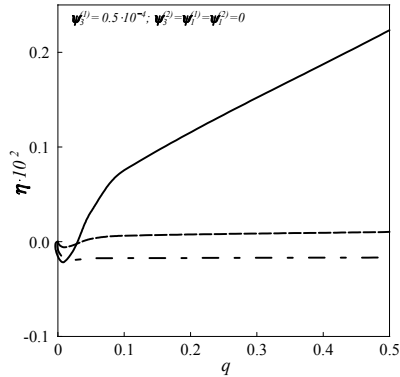


Figure 6: Normalized relative velocities η_{11} , η_{12} and η_{13} vs q for different levels of normalised residual stress $\psi_3^{(1)}$ for C1 composition

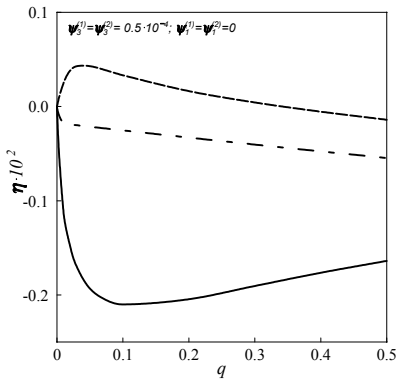


Figure 7: Relative velocities as a function of the thickness ratio q in the presence of two equal normalized residual stresses $\psi_3^{(1)} = \psi_3^{(2)}$ in both conductive and adhesive layers for C1 composition

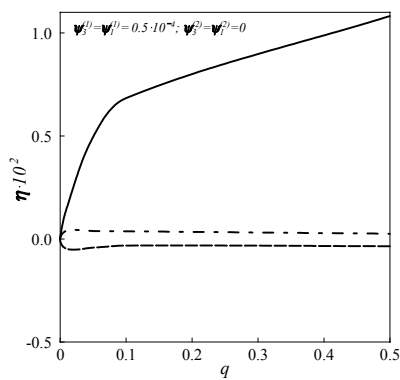


Figure 8: Relative velocities as a function of the thickness ratio q in the presence of two equal components of normalised residual stress $\psi_3^{(1)} = \psi_1^{(1)}$ in the conductive layer and zero pre-stress in the adhesive layers for C1 composition

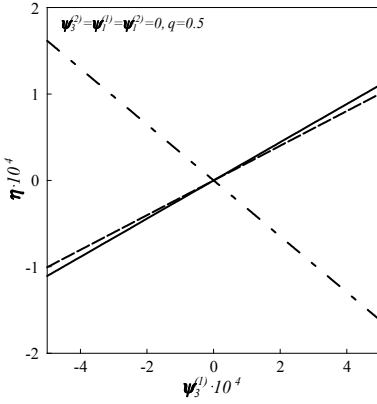


Figure 9:

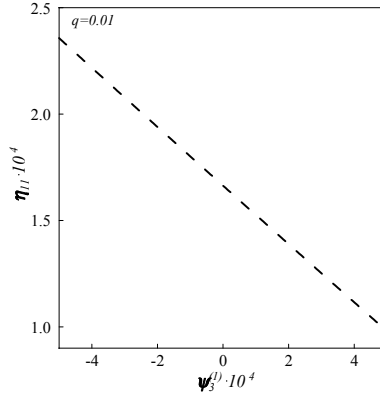


Figure 10: Normalized relative velocity η_{11} as a function of normalised residual stress $\psi_3^{(1)}$ for $q = 0.01$.

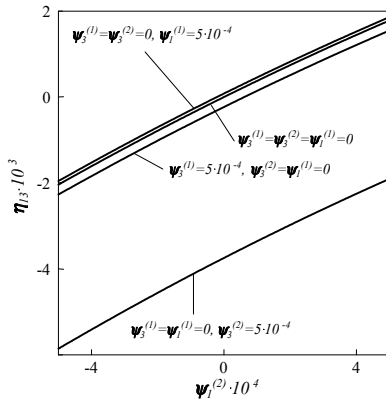


Figure 11: Dependence of η_{13} on normalised residual stress $\psi_1^{(2)}$ for different combinations of $\psi_1^{(1)}$, $\psi_3^{(1)}$ and $\psi_3^{(2)}$.

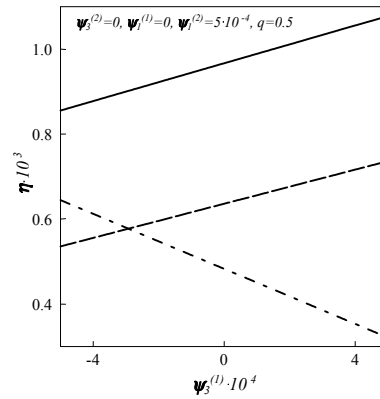


Figure 12: Normalized relative velocities η_{11} , η_{12} and η_{13} as the functions of $\psi_3^{(1)}$ for $\psi_3^{(2)} = \psi_1^{(1)} = 0$, $\psi_1^{(2)} = 5 \cdot 10^{-4}$, $q = 0.5$ for C1 composition

over the entire range of thickness ratios examined. It is evident that the behaviour of the curves remains the same and the relative velocities reach saturation faster at lower initial stresses.

The behaviour of the curves will not change if the stress $\sigma_{11}^{0(1)}$ is nonzero too. For the residual stresses that are compressive, all the curves can be obtained by mirror-

ing the curves for tensile stresses about the q -axis, which is completely consistent with the results obtained in [Zhuk, Guz (2006); Zhuk, Guz (2007)].

The pattern will change if the residual stresses $\sigma_{33}^{0(j)}$, $j = 1, 2$, are nonzero. Figure 6 presents the case where $\psi_3^{(1)} = 5 \cdot 10^{-4}$, $\psi_3^{(2)} = \psi_1^{(1)} = \psi_1^{(2)} = 0$. For small values of q the curves of η_{11} versus q and η_{13} versus q have local minima and the curves go through zero at $q \approx 0.026$. The relative velocity parameter η_{12} is negative over the whole interval of q . Both η_{12} and η_{11} become saturated very fast.

The above results indicate that under certain conditions and for special values of the thickness ratio of the layers, there are points $\eta_{11} = 0$ when transverse residual stresses are nonzero ($\sigma_{33}^{0(j)} \neq 0$, $\sigma_{11}^{0(j)} = 0$, $j = 1, 2$) and the curve of η_{13} versus q goes through zero when longitudinal residual stresses are nonzero ($\sigma_{33}^{0(j)} = 0$, $\sigma_{11}^{0(j)} \neq 0$, $j = 1, 2$). Other possible combinations of residual stress components may either strengthen or weaken this effect. For example, Fig. 7 shows the dependences of η on q for all the types of waves considered for $\psi_3^{(1)} = \psi_3^{(2)} = 5 \cdot 10^{-4}$, $\psi_1^{(1)} = \psi_1^{(2)} = 0$. It can be seen that the point $\eta_{11} = 0$ shifts towards $q \approx 0.35$.

Figure 8 illustrates the behaviour of relative velocities in the presence of both transverse and longitudinal residual stresses that are tensile in the metal layers and compressive in the adhesive layers ($\psi_3^{(1)} = \psi_1^{(1)} = 5 \cdot 10^{-4}$, $\psi_3^{(2)} = \psi_1^{(2)} = -5 \cdot 10^{-4}$). Here none of η_{11} , η_{12} or η_{13} is equal to zero over the considered range of the layer thickness ratio q .

Thus, the problem appears to be a multi-parameter one, with the magnitude and sign of residual stress components in layers having a combined effect. However, the type of the residual stress state in a multilayered structure and its internal pattern can be inferred from the behaviour of the dependences of η on q .

We also examine the influence of residual stresses on the behaviour of the relative velocities of plane waves in the multilayered structure under consideration. Typical results are presented in Figs. 9–12. Figure 9 illustrates the dependence of η on $\psi_3^{(1)}$ for $\psi_3^{(2)} = \psi_1^{(1)} = \psi_1^{(2)} = 0$ and $q = 0.5$. As can be seen, η_{12} decreases and η_{11} and η_{13} increase linearly with increase in the pre-stress, the curves going through zero at $\psi_3^{(1)} = 0$ (which represents a stress-free multilayered structure). These data are in good agreement with the results obtained in [Guz, Zhuk, Makhort (1976); Guz, Makhort (2000)]. Figure 10 shows η_{11} as a function of $\psi_3^{(1)}$ for $q = 0.01$. The relative velocity depends linearly on the residual stress for all the volume fractions of the multilayered structure constituents. For the relative velocities of quasi-shear and purely shear waves, the pattern is similar.

The effect of the second pre-stress components on the relative velocity of a quasi-

shear wave is illustrated by Fig. 11, which shows η_{13} as a function of $\psi_1^{(2)}$ for $-5 \cdot 10^{-4} \leq \psi_1^{(2)} \leq 5 \cdot 10^{-4}$ and different combinations of $\psi_1^{(1)}$, $\psi_3^{(1)}$ and $\psi_3^{(2)}$ such that only one of these parameters is nonzero. It is seen that with such residual stresses, the plots are again straight lines with a constant slope. The only difference is that the graphs slightly shift toward positive η_{13} when $\psi_3^{(1)} = \psi_3^{(2)} = 0$, $\psi_1^{(1)} = 5 \cdot 10^{-4}$ and toward negative η_{13} when $\psi_3^{(1)} = 5 \cdot 10^{-4}$, $\psi_3^{(2)} = \psi_1^{(1)} = 0$ §Ú $\psi_3^{(1)} = 0$, $\psi_3^{(2)} = 5 \cdot 10^{-4}$, $\psi_1^{(1)} = 0$. It appears that the velocity of the quasi-shear wave is most affected by the combination of the stresses $\sigma_{33}^{0(2)}$ and $\sigma_{11}^{0(2)}$.

For the other two relative velocities, the pattern is similar. Additional residual stress components cause the graphs to shift vertically. Sensitivity to one stress component or another is manifested differently under different conditions and should be analyzed under specific conditions.

Figure 12 shows η as a function of $\psi_3^{(1)}$ for $\psi_3^{(2)} = \psi_1^{(1)} = 0$, $\psi_1^{(2)} = 5 \cdot 10^{-4}$, and $q = 0.5$. This dependence can be obtained by rotating the curves for a pre-stress-free material with very small values of q (practically horizontal lines) about the origin through the angle corresponding to the chosen value of q (Fig. 10) and then translating them along the vertical axis (Fig. 11). Thus, having a table of angles of rotation corresponding to different values of q and a table of translations corresponding to different combinations and values of residual stress components, we can easily plot η versus ψ . Conversely, if we have these tabulated data and results of, say, acoustic tests, it will be possible to assess the level and type of residual stresses and to identify the internal pattern for the multilayered structure.

Similar analyses were performed for the other groups of multilayered structures from Table 2. Figures 13-16 present typical results for a representative of group II - the composition C6 (bronze plus EP-PS).

Figure 13 shows the relative velocities of quasi-compressional, quasi-shear, and purely shear waves as functions of the layer thickness ratio q for $\psi_1^{(1)} = 0$, $\psi_1^{(2)} = \psi_3^{(1)} = \psi_3^{(2)} = 5 \cdot 10^{-4}$. With such a distribution of pre-stresses, the velocities η_{13} and η_{11} monotonically increase, with η_{11} rapidly reaching saturation. The velocity η_{12} is always negative, rapidly decreasing at small q and meeting its saturated value of $0.1 \cdot 10^{-2}$.

The behaviour of relative velocities is qualitatively the same for $\psi_3^{(1)} = \psi_3^{(2)} = \psi_1^{(1)} = 5 \cdot 10^{-4}$, $\psi_1^{(2)} = 0$ (see Fig. 14). The only observable difference is that η_{11} is non-monotonic and does not meet its saturated value up to the $q = 0.5$. The maximum in the η_{11} vs q dependence is reached at $q \approx 0.75 \cdot 10^{-1}$. Then the relative velocity of the quasi-compressional wave decreases with the constant slope but does not become a zero in the considered range of q variations. Thus, the behaviour of the

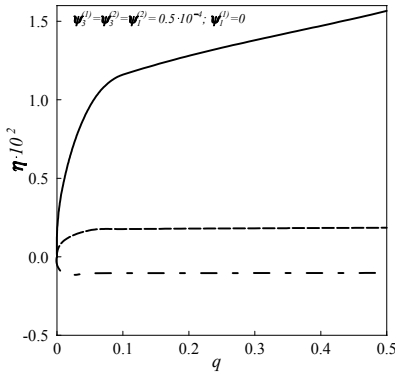


Figure 13: Normalized relative velocities of plane waves propagating along the Oz_1 -axis as a function of the thickness ratio of layers q in a multilayered structure with C6 composition for $\psi_1^{(1)} = 0, \psi_1^{(2)} = \psi_3^{(1)} = \psi_3^{(2)} = 5 \cdot 10^{-4}$

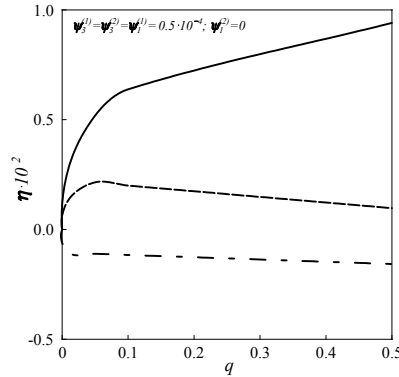


Figure 14: Normalized relative velocities of plane waves propagating along the Oz_1 -axis as a function of the thickness ratio of layers q in a multilayered structure with C6 composition for $\psi_1^{(2)} = 0, \psi_1^{(1)} = \psi_3^{(1)} = \psi_3^{(2)} = 5 \cdot 10^{-4}$

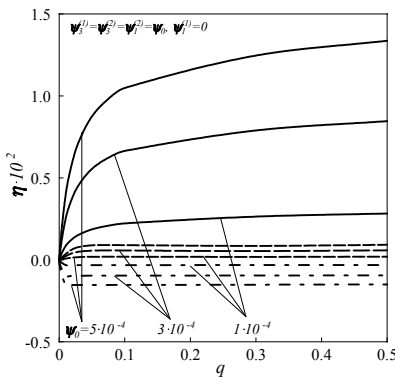


Figure 15: Effect of different levels of the pre-stress $\psi_3^{(1)} = \psi_3^{(2)} = \psi_1^{(2)} = \psi_0, \psi_1^{(1)} = 0$ on the relative velocities dependences on q for C6 composition

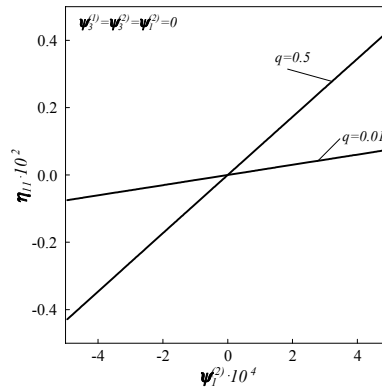


Figure 16: Normalized relative velocity η_{13} as a function of $\psi_1^{(1)}$ for $\psi_3^{(1)} = \psi_3^{(2)} = \psi_1^{(2)} = 0, q = 0.01$ and 0.5 for C6 composition

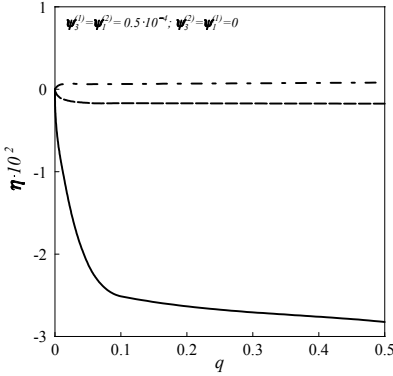


Figure 17: Normalized relative velocities of plane waves propagating along the Oz_1 -axis as a function of q for $\psi_3^{(1)} = \psi_1^{(2)} = 5 \cdot 10^{-4}$, $\psi_3^{(2)} = \psi_1^{(1)} = 0$ for C8 composition

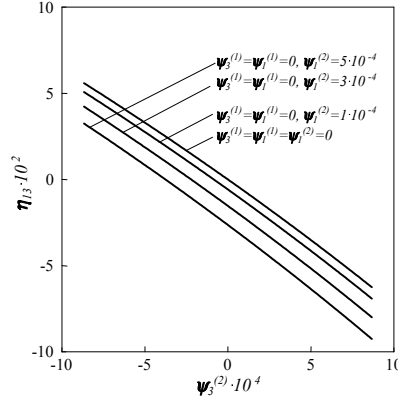


Figure 18: Relative velocity η_{13} as a function of $\psi_3^{(2)}$ for $q=0.5$ and different combinations of $\psi_1^{(1)}$, $\psi_1^{(2)}$ and $\psi_3^{(1)}$ for C8 combination

curves depends on which residual stress components are nonzero.

Figure 15 shows the dependence of the relative velocities of plane waves on the level of normalised residual stresses for $\psi_3^{(1)} = \psi_3^{(2)} = \psi_1^{(2)} = \psi_0$, $\psi_1^{(1)} = 0$. The values of ψ_0 are indicated near the curves. Changes in ψ_0 affect only the level of the curves, not their behaviour.

The behaviour of the graphs of η versus $\psi_i^{(j)}$ is qualitative similar to what was observed for the C1 composition. They are straight lines in all cases. Changes in q cause them to shift along the vertical axis. As an example, Fig. 16 shows η_{13} as a function of $\psi_1^{(1)}$ for $\psi_3^{(1)} = \psi_3^{(2)} = \psi_1^{(2)} = 0$ and the values of q equal to 0.01 and 0.5.

Further analysis reveals that the behaviour of the relative velocities of plane waves in nanocomposites of group III depends on $\psi_i^{(j)}$ and q in a similar manner as in the composites of groups I and II. Typical results for the C8 composition (brass + PMMA) are presented in Figs. 17 and 18. Figure 17 shows η as a function of q for $\psi_3^{(1)} = \psi_1^{(2)} = 5 \cdot 10^{-4}$, $\psi_3^{(2)} = \psi_1^{(1)} = 0$, and Fig. 18 shows η_{13} as a function of $\psi_3^{(2)}$ for $q=0.5$ and different combinations of $\psi_1^{(1)}$, $\psi_1^{(2)}$ and $\psi_3^{(1)}$. In all cases, the behaviour of curves is similar to that observed above for composites of other groups.

6 Concluding remarks

Following the analysis of numerical results, we can establish qualitative and quantitative patterns for stationary plane waves propagating along the layers in a multilayered structure in the presence of residual stresses. The relative velocities of quasi-compressional, quasi-shear, and purely shear waves are almost linearly dependent on residual stresses over the entire range examined. These velocities may be different in different multilayered structures. Residual stresses result in shift of the straight lines plotted for a structure without residual stresses along the vertical axis. For certain combination of residual stress components, a change in the thickness ratio of the layers, q , causes the originally horizontal line of η versus $\psi_i^{(j)}$ for a homogeneous material to rotate about the origin of coordinates.

On the other hand, the dependence of the velocities of plane waves on the thickness ratio q may be both monotonic and non-monotonic and its behaviour depends on the combination of residual stress components. The analysis of numerical results has revealed that for some multilayered structures there exists a thickness ratio, q , such that the velocity of a wave does not depend on the residual stresses and remains equal to the wave velocity in the corresponding multilayered structure without residual stresses.

The sign of residual stresses does not influence the behaviour of the curves of wave velocities versus the magnitude of this stress, but affects significantly the dependence of the velocity on the thickness ratio of the layers.

The relationships established here can be used in combination with the ultrasonic non-destructive methods [Guz, Zhuk, Makhort (1976); Guz (2001); Babich, Gluchov, Guz (2008a); Babich, Gluchov, Guz (2008b)] to assess the stress-strain state of multilayered structures for MEMS applications by processing experimental data. First, we need to know, according to [Guz (2001)], the density and the elastic moduli of the second and third orders of the materials of layers. Then, manufacturing-induced residual stresses can be estimated by measuring the difference in the velocities of longitudinal or transverse waves. Using a table of angles of rotation corresponding to different values of q and a table of translations corresponding to different combinations and levels of residual stress components, one can determine the level and type of residual stresses based on ultrasonic test data. The approach developed within the framework of continuum mechanics is applicable to the class of multilayered structures examined here owing to the use of the long-wave approximation in wave-propagation problems (i.e. a wave must be much longer than the typical length scale of the internal structure of the material). This fact can significantly simplify design of testing equipment, specimen preparation and experimental procedure.

Work is currently underway to examine the effect of diffusion processes on wave propagation in multilayered structures for MEMS applications. Interfaces between neighbouring materials are often subjected to diffusion processes which cause layers having gradually varying mechanical properties perpendicular to the interface. In contrast to previous work done in this field in which diffusion effects are generally considered as undesirable phenomena, studies [Kashtalyan, Menshykova (2007); Kashtalyan, Menshykova (2009a); Kashtalyan, Menshykova (2009b); Kashtalyan, Menshykova, Guz (2009);] have shown that presence of the layers with gradually varying material properties can significantly improve bonding in multilayered structures.

Acknowledgement: The financial support of the EPSRC (grant EP/E030351/1) and The Royal Society (International Joint Project) is gratefully acknowledged. The authors are very grateful to Prof. Igor Guz, Centre for Micro- and Nanomechanics, University of Aberdeen, for the helpful discussions and suggestions which contributed to the improvement of the paper.

7 References

- Akbarov, S.D.; Ozisik, M.** (2003): The influence of the third order elastic constants to the generalized Rayleigh wave dispersion in a pre-stressed stratified half-plane. *Int. J. Eng. Sci.*, vol. 41, pp. 2047-2061.
- Andrijasevic, D.; Smetana, W.; Esinenco, D.; Brenners, W.** (2006): Low temperature adhesive bonding in MEMS. In: W. Menz, S. Dimov and B. Fillon (eds) *Multi-Material Micro Manufacture*. Elsevier, Amsterdam, pp. 87-90.
- Babich, S.Y.; Gluchov, Y.P.; Guz, A.N.** (2008a): Dynamics of a prestressed incompressible layered half-space under moving load. *Int. Appl. Mech.*, vol. 44, pp. 268-285.
- Babich, S.Y.; Gluchov, Y.P.; Guz, A.N.** (2008b): A dynamic problem for a pre-stressed compressible layered half-space. *Int. Appl. Mech.*, vol. 44, pp. 388-405.
- Bettini, B.; Brusa, E.; Munteanu, M.; Specogna, R.; Trevisan, F.** (2008): Innovative numerical methods for nonlinear MEMS: the non-incremental FEM vs. the discrete geometric approach. *CMES: Computer Modeling in Engineering & Sciences*, vol. 33, pp. 215-242.
- Behrens, E.** (1967): Sound propagation in lamellar composite materials and averaged elastic constants. *JASA*, vol. 42, pp. 378-383.
- Brekhovskikh, L.M.** (1960): *Waves in Layered Media*. Academic Press, New York.

Brillouin, L.; Parodi, M. (1953): *Wave Propagation in Periodic Structures*. Dover Publ., New York.

Chakraborty, A. (2009): Wave propagation in porous piezoelectric media. *CMES: Computer Modeling in Engineering & Sciences*, vol. 40, pp. 105-132.

Guz, A.N. (1973): *Stability of Elastic Bodies under Finite Strains* [in Russian]. Naukova Dumka, Kiev.

Guz, A.N. (1999). *Fundamentals of the Three-Dimensional Theory of Stability of Deformable Bodies*. Springer-Verlag, Berlin.

Guz, A.N. (2001): On foundation of non-destructive method of determination of three-axial stress in solids. *Int. Appl. Mech.*, vol. 37, pp. 899-905.

Guz, A.N. (2002): Elastic Waves in Bodies with Initial (Residual) Stresses. *Int. Appl. Mech.*, vol. 38, pp.23-59.

Guz, A.N. (2004): *Elastic Waves in Bodies with Initial (Residual) Stresses* [in Russian]. A.S.K., Kiev.

Guz, A.N.; Han, L.M. (1976): Wave propagation in composite layered materials with large initial deformations, *Int. Appl. Mech.*, vol. 12, pp. 1-7.

Guz, A.N.; Makhort, F.G. (2000): The Physical Fundamentals of the Ultrasonic Nondestructive Stress Analysis of Solids. *Int. Appl. Mech.*, vol. 36, pp.1119-1149.

Guz, A.N.; Menshykov, O.V.; Zozulya, V.V.; Guz, I.A. (2007): Contact problem for the flat elliptical crack under normally incident shear wave. *CMES: Computer Modeling in Engineering & Sciences*, vol. 17, pp.205-214.

Guz, A.N.; Zhuk, A.P.; Makhort, F.G. (1976): *Waves in a Prestressed Layer* [in Russian]. Naukova Dumka, Kiev.

Han, L.M. (1977): Wave propagation along layers in initially strained laminated compressible materials. *Int. Appl. Mech.*, vol. 13, pp. 868-873.

Kashtalyan, M.; Menshykova, M. (2007): Three-dimensional elastic deformation of a functionally graded coating/substrate system. *Int. J. Solids Struct.*, vol. 44, pp. 5272-5288.

Kashtalyan, M.; Menshykova, M. (2009a): Three-dimensional elasticity solution for sandwich panels with a functionally graded core. *Compos. Struct.*, vol. 87, pp. 36-43.

Kashtalyan, M.; Menshykova, M. (2009b): Effect of a functionally graded interlayer on a three-dimensional elastic deformation of coated plates subjected to transverse loading. *Compos. Struct.*, vol. 89, pp.167-176.

Kashtalyan, M.; Menshykova, M.; Guz, I.A. (2009): Use of functionally graded layer to improve bonding in coated plates. *J. Adhesive Sci. Tech.*, vol. 23, pp.

1591-1601.

Kim, K.I.; Kim, J.M.; Hwang, G.C.; Baek, C.W.; Kim, Y.K. (2006): Packaging for RF MEMS devices using LTCC substrate and BCB adhesive layer. *J. Micromech Microeng.*, vol. 16, pp. 150-156.

Lee, W.M.; Chen, J.T. (2009): Scattering of flexural wave in thin plate with multiple holes by using the null-field integral equation approach. *CMES: Computer Modeling in Engineering & Sciences*, vol. 37, pp. 243-273.

Ljung, P.; Bachtold, M.; Spasojevic, M. (2000): Analysis of realistic large MEMS devices. *CMES: Computer Modeling in Engineering & Sciences*, vol. 1, pp. 21-30.

Menshykova, M.V.; Menshykov, O.V.; Guz, I.A. (2009): Linear Interface crack under plane shear wave. *CMES: Computer Modeling in Engineering & Sciences*, vol. 48, pp. 107-120.

Niklaus, F.; Enoksson, P.; Kalvesten, E.; Stemmes, G. (2001): Low-temperature full wafer adhesive bonding. *J. Micromech. Microeng.*, vol. 11, pp.100-107.

Pang, C.; Zhao, Z.; Du, L.; Fang, Z. (2008): Adhesive bonding with SU-8 in a vacuum for capacitive pressure sensors. *Sensors and Actuators A*, vol. 147, pp. 672-676.

Romanowicz, B.F.; Zaman, M.H.; Bart, S.F.; Rabinovich, V.L.; Tchertkov, I.; Zhang, S.; da Silva, M.G.; Deshpande, M.; Greiner, K.; Gilbert, J.R.; Cunningham, S. (2000): A methodology and associated CAD tools for support of concurrent design of MEMS. *CMES: Computer Modeling in Engineering & Sciences*, vol. 1, pp. 45-64.

Sadaba, I.; Fox, C.H.J.; McWilliam, S. (2006): A study of residual stress effects due to adhesive bonding of MEMS components. *Applied Mechanics and Materials*, vol. 5-6, pp. 493-500.

Satyanarayana, S.; Karnik, R.N.; Majumdar, A. (2005): Stamp-and-stick room-temperature bonding technique for microdevices. *J. Microelectromechanical Systems* vol. 14, pp. 392-399.

Spearing, S.M. (2000): Materials issues in microelectromechanical systems (MEMS), *Acta Mater.*, vol. 48, pp.179-196.

Wei, J.; Su, X. (2009) Steady-state response of the wave propagation in a magneto-electro-elastic square column. *CMES: Computer Modeling in Engineering & Sciences*, vol. 37, pp. 65-84.

Ye, W.; Mukherjee, S. (2000): Design and fabrication of an electrostatic variable gap comb drive in micro-electro-mechanical systems. *CMES: Computer Modeling in Engineering & Sciences*, vol. 1, pp. 111-120.

Zhuk, Y.A.; Guz, I.A. (2006): Influence of prestress on the velocities of plane

wave propagating normally to the layers of nanocomposites. *Int. Appl. Mech.*, vol. 42, pp. 729-744.

Zhuk, Y.A.; Guz, I.A. (2007): Features of plane wave propagation along the layers of a prestrained nanocomposite. *Int. Appl. Mech.*, vol. 43, pp. 361-379.